Impacts of Anomalous Midlatitude Cyclone Activity over East Asia during Summer on the Decadal Mode of East Asian Summer Monsoon and Its Possible Mechanism

HAISHAN CHEN

Collaborative Innovation Center on Forecast and Evaluation of Meteorological Disasters/Key Laboratory of Meteorological Disaster, Ministry of Education, and International Joint Research Laboratory on Climate and Environment Change, and School of Atmospheric Sciences, Nanjing University of Information Science and Technology, Nanjing, China

FANGDA TENG AND WANXIN ZHANG

School of Atmospheric Sciences, Nanjing University of Information Science and Technology, Nanjing, China

HONG LIAO

International Joint Research Laboratory on Climate and Environment Change, and School of Environmental Science and Engineering, Nanjing University of Information Science and Technology, Nanjing, China

(Manuscript received 23 February 2016, in final form 27 September 2016)

ABSTRACT

By using an objective identification and tracking algorithm of the cyclone, the statistics of midlatitude cyclone activity in East Asia during summer for the period 1979–2013 were analyzed. The impact of the midlatitude summer cyclone anomalies in East Asia on the decadal mode of East Asian summer monsoon (EASM) was investigated and possible mechanisms were proposed. The possible reasons for the anomalous cyclone activity from the perspective of land surface thermal forcing were also explored. Results indicate that the midlatitude summer cyclone activity over East Asia exhibits decadal changes in the period of 1979–2013 and is significantly weakened after early 1990s. Further analysis indicates that there is a close relationship between the midlatitude summer cyclone activity over East Asia and the decadal variation of EASM; when the midlatitude summer cyclone activity over East Asia is strong (weak), EASM tends to be intensified (weakened), and the weak cyclone activity after 1993 generally coincides with the decadal weakening of EASM. Moreover, there is a close linkage between the weakening of cyclonic activity after the early 1990s and the nonuniform surface warming of the Eurasian continent. Significant warming to the west of Mongolia tends to weaken the north–south temperature gradient and the atmospheric baroclinicity to its south and eventually can lead to weakening of the midlatitude cyclone activity over East Asia.

1. Introduction

East Asia is one of the regions significantly affected by monsoon activities, and anomalies of the East Asian summer monsoon (EASM) are closely related to severe climate disasters (such as droughts, floods, and extremely high temperatures in China). Therefore, the variability of EASM has been paid great attention in recent decades, and the mechanisms of its formation, evolution, and variation have been widely investigated (Tao and Chen 1987; Ding and Chan 2005; He et al. 2007b; Huang et al. 2012; Hsu et al. 2014). Previous studies indicated that EASM exhibits multiscale characteristics of temporal and spatial variability. Huang et al. (2012) noted that EASM has a quasi-biennial oscillation and an evident longitudinal tripole spatial pattern. On a decadal time scale, abrupt change of EASM occurred at the end of 1970s: EASM has been significantly weakened and accompanied by an increase of rainfall in the Yangtze River basin of China and

Denotes Open Access content.

Corresponding author e-mail: Haishan Chen, haishan@nuist.edu.cn

DOI: 10.1175/JCLI-D-16-0155.1

decrease of rainfall in northern China (Wang 2001; Ding et al. 2008, 2009). In addition, recent studies suggested that a significant decadal variation of EASM happened in the early 1990s (Ding et al. 2008, 2009; Wu et al. 2009b). Corresponding to the decadal variation of EASM, there is also evidence of associated summer atmospheric circulation and climate in East Asia, including significant weakening of the subtropical westerly jet (Kwon et al. 2007) and the north–south temperature gradient in the troposphere (Zhang and Zhou 2015), as well as significant increases of the summer rainfall in southern China (Wu et al. 2010).

Despite significant progress in understanding the variation of EASM, its mechanism is still far from well understood owing to the intrinsic complexity of the EASM system. EASM is affected by not only the tropical and subtropical monsoon circulations (Chang et al. 2000a,b; Wang et al. 2000, 2008) but also the mid- to high-latitude circulation and the associated cold air activity (He et al. 2007a; Ding and Wang 2007). From the perspective of external atmospheric forcing, other components of the climate system (e.g., ocean and land surface) are also closely related to the variability of EASM (Wang et al. 2000; Huang et al. 2003; Wu et al. 2004, 2009a,b; Zhang and Zuo 2011).

EASM significantly differs from the Indian summer monsoon in that it is closely related to the mid- to high-latitude circulation system. The warm and moist air from the south moves northward and encounters the cold air from the mid- to high latitudes, resulting in the mei-yu front rainfall (Tomita et al. 2011; Seo et al. 2015). The duration and amount of rainfall during the mei-yu period are related to the position, intensity, and water vapor transport of the tropical circulation system and are also affected by the mid- to high-latitude circulation (Tao and Chen 1987). So far, few studies have focused on the influences of the mid- to high-latitude circulation system on EASM. It has been suggested that the impact of anomalous atmospheric circulation in the mid- to high latitudes during summer on the weather and climate over East Asia is mainly reflected by the blocking high and abnormal latitudinal teleconnection wave trains (Wu 2002; Fujinami and Yasunari 2009; Seo et al. 2012; Park et al. 2015). However, very limited studies have been reported on the relationship between the cyclone activity in the mid- to high latitudes and the EASM as well as the related mechanisms.

The mid- to high-latitude area of the Eurasian continent has experienced the most intensive warming in the past several decades (Hansen et al. 2006, 2010). Recent studies have found that there is a very strong spatial heterogeneity in the variation of the surface temperature over the Eurasian continent and that the strongest warming appears in northwestern Asia (i.e., southeast of Russia, Mongolia, and north of China). An evident decadal variation in the surface temperature over this region occurred after the early 1990s (Qi and Wang 2012; Chen and Lu 2014). The midlatitude cyclone is a low pressure vortex with strong baroclinicity that occurred in the mid- to high latitudes in the Southern and Northern Hemispheres. In the context of global warming, changes of the surface temperature can have a significant impact on the generation and movement of cyclones (McCabe et al. 2001; Lehmann et al. 2014). Previous studies showed that significant changes in the cyclone activity and atmospheric circulation over East Asia have occurred over the past decades (Wang et al. 2009; Zhang et al. 2012a). The variation of such circulation anomalies can also lead to anomalous EASM activity (Park et al. 2015) and further affect the East Asian climate (Zhu et al. 2012; Coumou et al. 2015). Therefore, in the current study, the possible connection between the midlatitude cyclone activity over East Asia during summer and the EASM as well as the relevant physical mechanisms was investigated. We also explored the possible linkage between the anomalous midlatitude cyclone activity and the nonuniform land surface warming.

The remaining sections of this paper are structured as follows. Section 2 describes the data and methods used in this study, and section 3 focuses on the variation of the midlatitude cyclone activity. Section 4 presents discussion on the relationship between the cyclone activity and EASM together with the relevant physical mechanisms. Further discussion on the possible linkage between anomalous midlatitude cyclone activity and land surface warming is given in section 5, followed by conclusions in section 6.

2. Data and methods

Data used in this study are from the European Centre for Medium-Range Weather Forecasts interim reanalysis (ERA-Interim; Dee et al. 2011; http://apps.ecmwf.int/datasets/) and the National Centers for Environmental Prediction–National Center for Atmospheric Research (NCEP–NCAR) reanalyses (Kalnay et al. 1996; http://www.esrl.noaa.gov/psd/), including 4-times-daily (ERA-Interim) and daily (NCEP–NCAR reanalyses) and monthly sea level pressure, geopotential height, and meridional and zonal wind speed. The temperature data used include monthly average surface temperature at 2 m from ERA-Interim, NCEP–NCAR reanalyses, and the Climatic Research Unit (CRU) Time Series, version 3.2.2 (hereafter the dataset is referred to as CRU), of the University of East Anglia in the United Kingdom (Harris et al. 2014; http://www.cru.uea.ac.uk/data/), and the monthly average surface

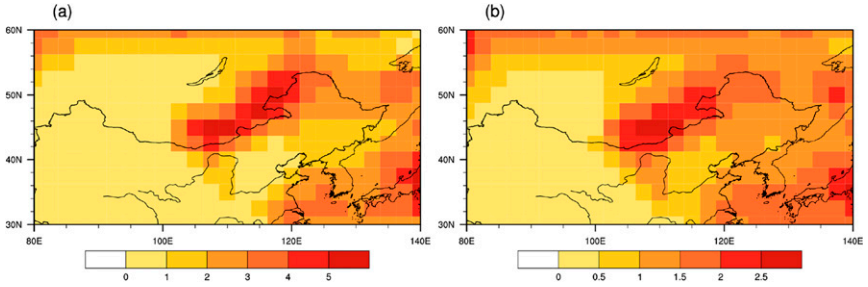

FIG. 1. Geographic distributions of (a) climatology and (b) interannual variability (std dev) of the midlatitude cyclone activity frequency (number of cyclone centers in a 2.5° × 2.5° grid) in summers (JJA) over East Asia during 1979–2013.

temperature from the National Aeronautics and Space Administration Goddard Institute for Space Studies (NASA GISS; Hansen et al. 2010; http://data.giss.nasa.gov/gistemp/). The monthly precipitation data are from the Global Precipitation Climatology Project (GPCP; Adler et al. 2003). The spatial resolution is 0.5° × 0.5° for the CRU surface temperature data 2° × 2° and 2.5° × 2.5° for other data, and the time period investigated is 35 years (1979–2013).

In this study, an objective identification and tracking algorithm of the cyclone is used to acquire the statistics of the cyclone activity based on the 4-times-daily sea level pressure data. The method was proposed by Murray and Simmonds (1991a,b) and refined by Simmonds et al. (1999). Details are as follows. First, we determine the position of the maximum Laplacian of the sea level pressure and search for the minimum local pressure in its vicinity, which is defined as the center of cyclone at current time step t. Second, based on the locations of the cyclone center at time step t, we estimate the location of the cyclone at the next time step $t + 1$ by extrapolation according to the moving velocities of the steering flow and the cyclone itself. The authentic cyclone center in the most probable combination with the estimated center at time step $t + 1$ in its vicinity is assumed to be moved from the center at previous time step t. If we cannot find such a center, the cyclone is assumed to have dissipated. If we cannot find a center at the previous time step, the cyclone can be regarded as nascent. To reduce the error of using the local minimum sea level pressure as the criterion to identify cyclones in high-elevation areas, we set a height threshold to eliminate cyclone activity in regions where the elevation is greater than 1500 m.

3. Variation in the midlatitude cyclone activity over East Asia

First, we used the objective identification and tracking algorithm of the cyclone to establish data of cyclone paths in 1979–2013 and defined the numbers of cyclone tracks passing a grid cell of 2.5° longitude × 2.5° latitude during summer (with repeated entries of the same track being counted as one) as the frequency of cyclone activity, which is used to characterize the midlatitude cyclone activity in East Asia. Figure 1a shows the average frequency of summer cyclone activity over 35 years in the northern part of East Asia. Since the cyclone activity in areas with elevations over 1500 m was excluded, there is generally no significant cyclone activity in the high-elevation region to the west of Mongolia. The maximum of cyclone activity mainly appears in midwestern Mongolia and northeastern China. High frequency of the cyclone activity generally exhibits a zonal pattern and slightly slants to the northeast, indicating that the cyclones move eastward from central Mongolia to north of Heilongjiang in China. These results are generally consistent with the basic characteristics of the average frequency of the summer cyclone activity in the Northern Hemisphere from 1958 to 2001 as described by Zhang et al. (2012a) using ERA-40 data. Figure 1b shows the interannual variability of the frequency of cyclone activity. The maximum standard deviation of cyclone activity is also located in central Mongolia, which indicates that both the most frequent cyclone activity and the greatest variation of cyclone activity happen in this area. Therefore, in the following analysis, Mongolia was selected as the representative area for the midlatitude cyclone anomaly activity in East Asia.

To further discuss the general variation in the midlatitude cyclone activity over East Asia, we define the total number of East Asia midlatitude summer cyclones (EAMC) as the number of cyclones with more than half of their lifetimes (results are similar when we change the criteria to one-third or two-thirds; figures not shown) in the representative area (40°–50°N, 80°–140°E). To exclude the impact of the seasonal and local geothermal low, we eliminated cyclones with lifetimes less than 12 h (Wang et al. 2009). If not specified, the cyclones

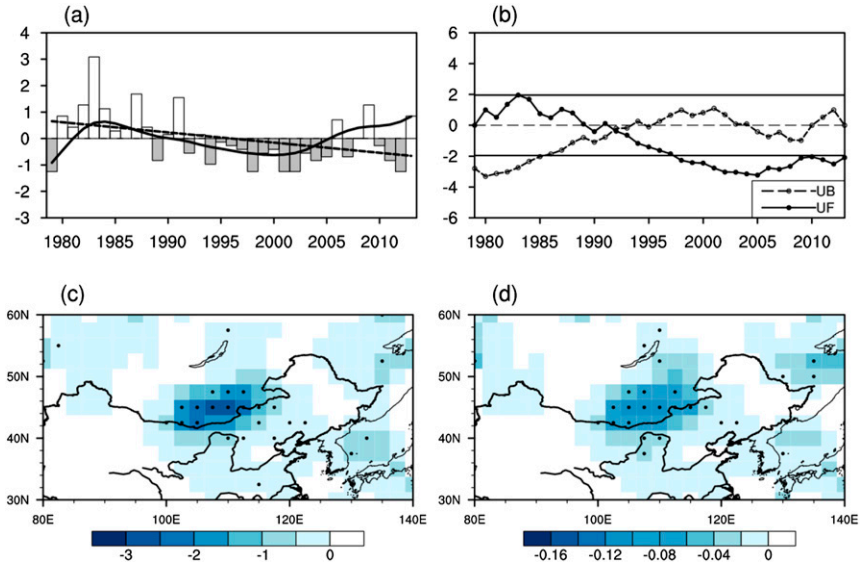

FIG. 2. (a) Standardized departures of the number of EAMC (bars) with the linear trend (dashed line) and result of 11-point Gaussian filter after removing linear trend (solid line). (b) MK statistical test (marked lines; UF is forward sequential statistic, while UB is backward sequential statistic) with horizontal solid lines indicating values passing the 5% significance level. (c) Difference of summer (JJA) midlatitude cyclone activity frequency between periods of 1994–2013 and 1979–93 (counts per grid). (d) Linear trend of the midlatitude cyclone activity frequency (counts per grid per year). Black dots denote regions where differences and linear trends are statistically significant at the 5% level.

discussed in this paper refer to the midlatitude cyclones in East Asia. The histogram in Fig. 2a shows the time series of the normalized number of cyclones in the representative area. A significant weakening trend in the cyclone activity occurred during 1979–2013 (dashed line in Fig. 2a), which passes the significance test at the 5% level. By removing the linear trend, we conducted an 11-point Gaussian filtering of the time series of the cyclone number (solid line in Fig. 2a) and found that there was also a significant signal of decadal variation in the cyclone activity. Results of the Mann–Kendall (MK) statistical test (Fig. 2b) indicate that since the early 1990s, there has been a significant weakening of cyclone activity; there is also a significant difference in the cyclone activity before and after 1993.

Figure 2c shows the composite difference in the frequency of cyclone activity before and after 1993. The cyclone activity to the north of East Asia decreased significantly after 1993, and the greatest decrease occurred in central Mongolia. Zhang et al. (2012b) studied the variation in the frequency of cyclone generation in East Asia and divided the midlatitude cyclones into two categories (i.e., southern cyclones and northern cyclones) based on the locations of their sources. They found that the generation of northern cyclones decreased significantly after 1990, which is consistent with the results of the current study. Figure 2d shows the spatial distribution of the linear trend of the cyclone activity, which is similar to Fig. 2c. It can be concluded that the significant weakening of the cyclone activity in central Mongolia is closely related to its decadal variation after 1993.

4. Relationship between cyclone activity and the decadal mode of EASM and its possible mechanism

a. Relationship between cyclone activity and the decadal mode of EASM

Cyclones are the main synoptic systems in the mid- to high latitudes. There has been a significant change in cyclone activity over the past 35 years, and abnormal activity can affect the local weather and climate. To investigate the possible relationship between cyclone activity and EASM, we selected the years with typical cyclone activity for the composite analysis. Based on the normalized indices of the cyclone number in the representative area, years with indices greater than 1 (i.e., 1982, 1983, 1984, 1987, 1991, and 2009) are selected as strong cyclone activity years, while years with indices less than −1 (i.e., 1979, 1998, 2001, 2002, and 2012) are weak

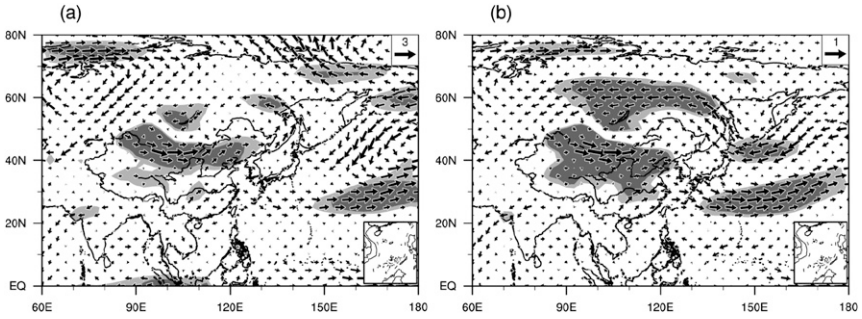

FIG. 3. (a) Composite (strong EAMC minus weak EAMC years) of 850-hPa horizontal winds ($m\,s^{-1}$) over Eurasia and (b) regression of 850-hPa horizontal winds anomaly ($m\,s^{-1}$) onto the normalized EAMC time series, in which the dark (light) shaded areas are statistically significant at the 5% (10%) level.

cyclone activity years. Figures 3a and 3b show the composite difference of 850-hPa horizontal winds (strong minus weak cyclone activity years) and regression of 850-hPa horizontal wind anomaly onto the normalized cyclone numbers, respectively. The circulation patterns are basically similar. A weak anomalous anticyclonic circulation exists in the southeast coastal area of China and a strong anomalous cyclonic circulation appears near Lake Baikal, resulting in a consistent anomalous southerly from low to high latitudes in eastern China. Our results are well supported by a recent study of Park et al. (2015), which carefully examined the effect of the anomalously low surface pressure propagating southeastward from Mongolia/northern China to far East Asia on monsoon precipitation.

Huang et al. (2015) used the low-level wind field to describe the anomalous monsoon activity and revealed the multimode spatial characteristics of the EASM anomaly. The method used to extract the dominant spatial modes of EASM is similar to the multivariate EOF (MV-EOF) in Wang et al. (2008), while only meridional and zonal winds at 850 hPa in East Asia (10°–60°N, 100°–140°E) are decomposed to reflect the variation of summer monsoon circulation in the current study. The first and second modes account for 19.8% and 14.9% of the total variance, respectively. The first mode of the East Asian summer monsoon [EASM principal component 1 (EASM-PC1)] is characterized by enhanced southwesterly monsoon from southern China to the middle and lower reaches of the Yangtze River and strengthened easterly anomalies between 10° and 20°N. The spatial patterns of the anomalous precipitation related to EASM-PC1 show a north–south dipole pattern with dry anomalies over the northern South China Sea and Philippine Sea and enhanced precipitation along the Yangtze River valley to southern Japan (Fig. 4a). The leading mode mainly reflects the interannual variation, while the second mode shows a pattern distinct from the first one and exhibits evident decadal variation. Actually, the decadal variation of EASM given by the second mode of EASM has been reported by several other studies (Ding et al. 2008, 2009; Wu et al. 2009b). As shown in Fig. 4b, the atmospheric circulation anomalies corresponding to the second mode of the East Asian summer monsoon [EASM principal component 2 (EASM-PC2)] are featured by a strong cyclonic anomalous circulation over regions to the east of Lake Baikal. In addition, there is an anomalous southwesterly wind to the southeast of the cyclonic circulation, which reflects the strengthening of the summer monsoon, especially in northern China. The spatial pattern of precipitation anomalies associated with EASM-PC2 shows a dipole pattern with suppressed rainfall over southern China and enhanced precipitation in northern and northeastern China (shaded in Fig. 4b).

Compared with Fig. 3, it is noted that the atmospheric circulation anomaly related to the cyclone activity is generally consistent with the second mode of EASM. Such an anomalous circulation pattern indicates that strong (weak) cyclone activity tends to be associated with an anomalous cyclonic (anticyclonic) circulation pattern, which favors the enhancement (weakening) of the southwesterly to the southeast of the anomalous circulation. Figure 4c shows that the time coefficient for the second mode of EASM changed from positive before 1993 to negative after 1993 and exhibits a significant weakening trend from 1979 to 2013 (passing the significance test at the 5% level). By removing the linear trend in this time series and performing 11-point Gaussian filtering, we find a significant signal of decadal variation of EASM. Results of the MK test (Fig. 4d) also indicate a significant weakening trend of EASM since the early 1990s that has been more significant

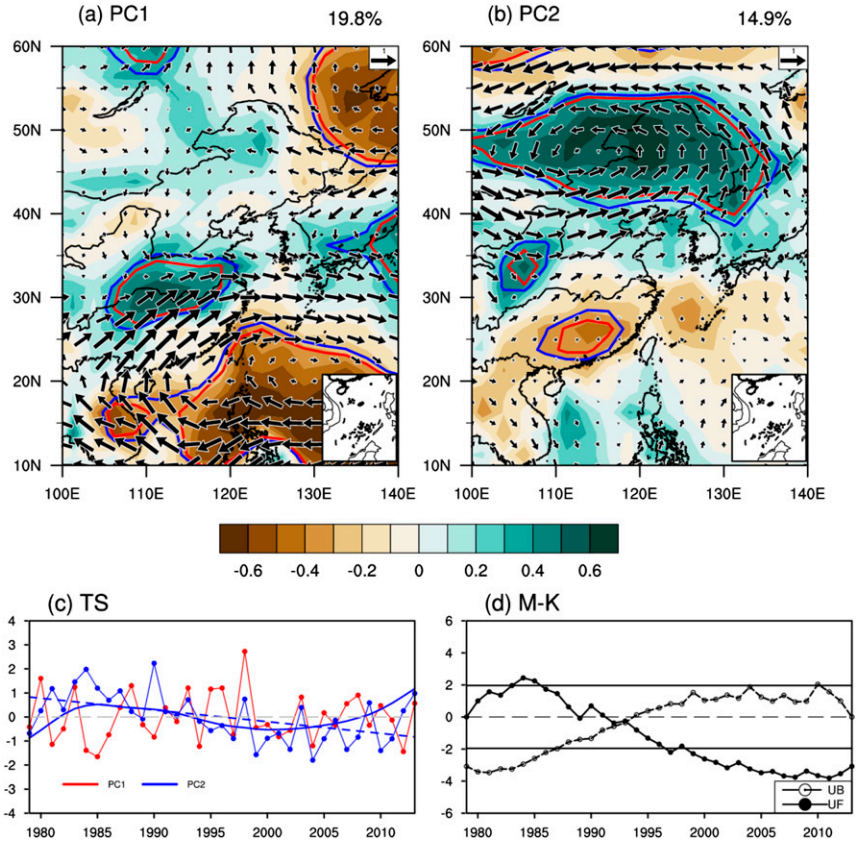

FIG. 4. Spatial pattern (m s^{-1}; vectors) of the (a) first and (b) second mode of EASM, which are given by the first two modes of the summer 850-hPa wind EOF analysis over East Asia. The correlation coefficients between time series of PC1 (PC2) and precipitation are shaded in (b), and the red (blue) contours indicate that the coefficients pass the statistical test at the 5% (10%) significance level. (c) Time series (marked lines) of the first (red) and second (blue) modes of EASM (solid line shows 11-point Gaussian filtered results and dashed line shows the linear trend of the time series of PC2). (d) Mann–Kendall statistical test (marked lines), in which the horizontal solid lines indicate the values passing statistical test at the 5% significance level. UF is forward sequential statistic, while UB is backward sequential statistic.

after the mid-1990s (significant at the 5% level). It also suggests that significant decadal variation of EASM happened around 1993, after which EASM is weakened and the low-level southwesterly in East Asia exhibits a consistent weakening. Since both cyclone activity and EASM exhibit similar decadal changes, we only focused on the decadal mode of EASM as well as its relationship with the anomalous cyclone activity during the past 35 years.

To more directly characterize the relationship between the cyclone activity and the decadal variation of EASM, Fig. 5a presents their time series over 35 years. There is a significant positive correlation between the two series (correlation coefficient of 0.59, which becomes 0.50 after removing the linear trend). The averages of the two time periods of 1979–93 and 1994–2013 (dashed line in Fig. 5a) show that EASM and cyclonic activity both exhibit significant differences before and after 1993. We further selected 9 (dashed line) and 10 years (solid line) as moving windows to conduct moving Student's *t* tests on the two time series (Fig. 5b), which both show changes in 1993; the changes pass the significance test at the 1% level and do not depend on the selection of the moving window, which is consistent with the results of the MK test. In summary, there is a significant positive correlation between the cyclone activity in the midlatitudes of East Asia and EASM, and both of them exhibit significant decadal weakening in early 1990s.

b. *Possible mechanisms accounting for the impacts of cyclone activity on EASM*

Figure 6 depicts the spatial distribution of the sea level pressure and the geopotential height anomaly at 500 and 300 hPa, which was derived from the regression of the

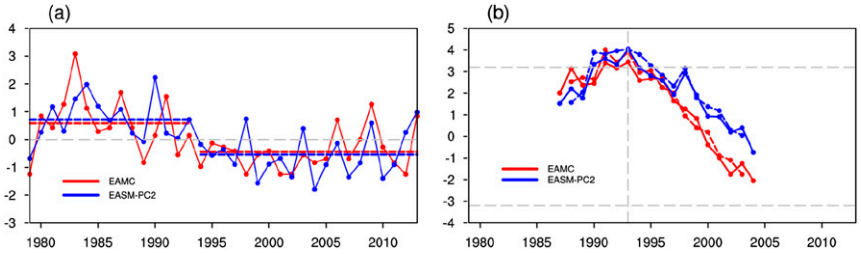

FIG. 5. (a) Normalized time series of EAMC and EASM (marked lines), where horizontal dashed lines indicate the average during 1979–93 and 1994–2013, respectively. (b) Statistics of the moving Student's *t* test for EAMC and EASM during 1979–2013, in which solid and dashed marked lines are results for a 9- and 10-yr window, respectively. Horizontal dashed gray lines indicate the values passing statistical test at the 1% significance level, and the vertical dashed gray line shows the significant abrupt changing point.

normalized number of cyclones. As shown in Figs. 6a and 6b, when the cyclone activity is abnormally strong, a large area of positive sea level pressure anomalies appears in the high-latitude area to the north of 60°N over the Eurasian continent, which extends over the West Siberian Plain, the Central Siberian Plateau, and most areas of the Russian Far East. A negative anomaly is located in Mongolia to the south of Lake Baikal and northeastern China and in particular to the east of Mongolia and in the central area of Mongolia in China, which passes the significance test at the 5% level. A positive sea level pressure anomaly is also found at low latitudes near Indochina, the South China Sea, the southeastern coastal area of China, and a large area to the east of the Philippines Archipelago, which however does not pass the significance test at the 5% level. Figures 6c and 6d show that the 500-hPa geopotential height anomaly field has three anomaly centers in the midlatitudes of the Eurasian Continent, with two positive anomaly centers located on the west side of the Ural Mountains and to the north of the Okhotsk Sea, and a negative anomaly center located to the south of Lake Baikal. The locations of these anomaly centers correspond to those of the anomalies of the sea level pressure. These results indicate that in years with relatively strong cyclone activity, the blocking high in the Ural Mountains and the Okhotsk Sea is strong, and there exists significant abnormal low pressure in the Lake Baikal area. The 300-hPa geopotential height anomaly also shows an anomalous pattern that is similar to the sea level pressure and 500-hPa geopotential height, but with stronger intensity (Figs. 6e,f). The atmospheric circulation anomaly in East Asia exhibits consistent variations in the upper, middle, and lower troposphere, which indicates that the atmospheric circulation anomaly associated with anomalous cyclone activity shows a quasi-barotropic structure and that the dynamic effect could play a dominant role. In the following discussion, by diagnosing the synoptic-scale physical variables related to the anomalous cyclone activity, we further investigated the possible mechanism by which the cyclone activity affects the atmospheric circulation in East Asia.

Both the identification and tracking methods of individual cyclone (Ulbrich et al. 2009) and bandpass filter methods (Chang et al. 2012) have been used to analyze the activity of extratropical storms, and it is conceivable that the cyclone frequency and storm tracks are highly consistent in their spatial pattern and temporal variations. From the perspective of the development of baroclinic wave activity, the cyclone activity generally consists of two stages (i.e., wave growth and maturity to dissipation of the waves). The stage of wave growth is usually accompanied by a very strong poleward and upward temperature flux, which mainly reflects the baroclinic conversion of the effective potential energy to the transient kinetic energy of the waves. In the stage of maturity to dissipation of the waves, the temperature flux decreases significantly, while the barotropic decaying process related to the conversion of transient kinetic energy of the wave to the zonal mean kinetic energy plays a dominant role. The cyclone is generated at the west end of the storm track and dissipates at the eastern end, and the actions of the poleward temperature flux and the momentum flux during the dissipation stage convert the transient kinetic energy of the cyclone to the kinetic energy of the mean flow. Therefore, the feedback of the synoptic-scale transient wave activity in the storm-track area on the mean flow can be used to describe the impact of the cyclone activity on the large-scale circulation.

Lau and Nath (1991) used the quasigeostrophic potential vorticity equation to decompose the roles of the transient wave activity on the mean flow into two categories, the vorticity flux and the heat flux, and noted that their impacts on the geopotential tendency of the mean

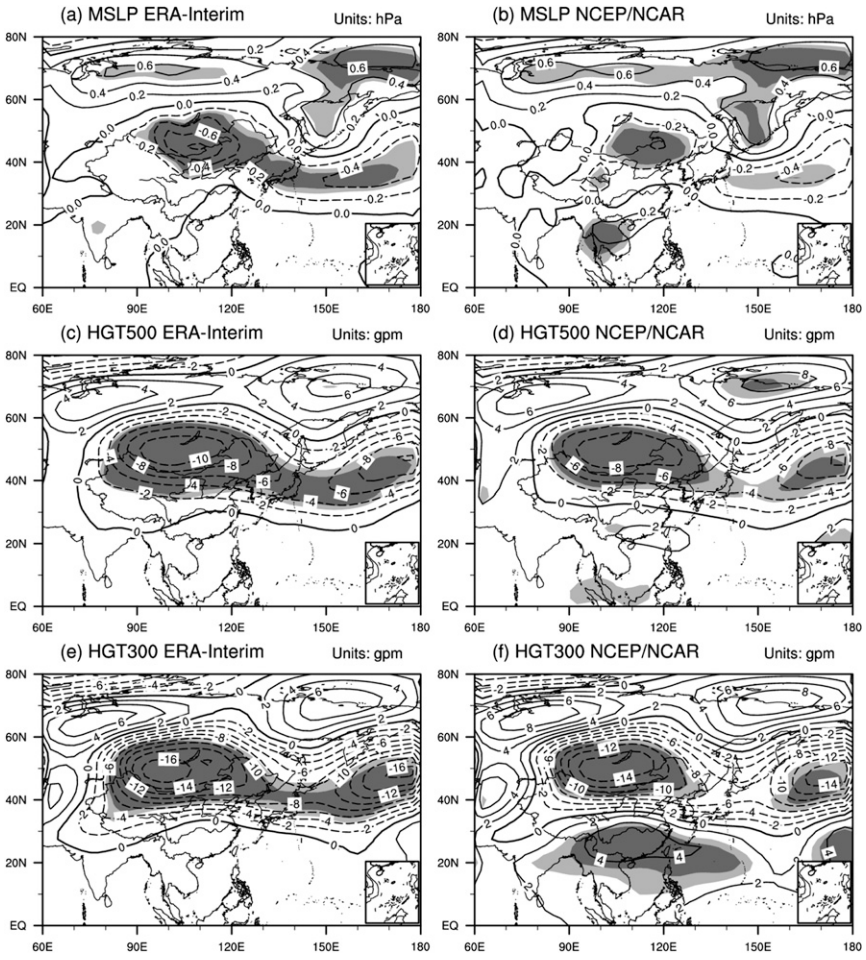

FIG. 6. (a),(b) Regressions of summer mean sea level pressure anomalies (hPa) and (c),(d) 500- and (e),(f) 300-hPa geopotential height anomalies (gpm) onto the normalized EAMC time series based on (left) ERA-Interim and (right) NCEP–NCAR reanalyses data, in which dark (light) shading denotes the regions where the regression is statistically significant at the 5% (10%) level.

flow are consistent at low levels and opposite at high levels. When the geopotential height anomalies at low levels are consistent with those at high levels (Fig. 6), the vorticity flux is the dominant contributor to the impact of the cyclone activity on the large-scale circulation. Previous studies (Lau and Holopainen 1984; Lau 1988) have suggested that the strength of the dynamic effect of the synoptic-scale atmospheric transient forcing can be expressed by the poleward eddy vorticity flux (PEVF) $\overline{v'\xi'}$, while the impact of the synoptic transient dynamic forcing (STDF) on the mean flow can be expressed by the time-averaged geopotential tendency, which has been used to diagnose the possible feedback of eddies on the intraseasonal variations of the East Asian trough (Song et al. 2016). Moreover, the horizontal Eliassen–Palm (EP) flux E_u and its divergence can be used to describe the interaction between the synoptic-scale wave and the low-frequency flow in barotropic cases. The divergence area of the EP flux usually corresponds to the acceleration of the westerly jet, with the northern side corresponding to the anomalous cyclonic circulation and the southern side corresponding to the anomalous anticyclonic circulation. The opposite situation occurs in the convergence area of the EP flux (Trenberth 1986). The STDF and the horizontal EP flux can be calculated using the following equations:

$$\mathrm{STDF} = -\frac{f}{g}\nabla_h^{-2}[\nabla_h \cdot \overline{(v'\xi')}] \quad \text{and} \tag{1}$$

$$E_u = \left[\frac{1}{2}(v'^2 - u'^2)\mathbf{i}, -\overline{u'v'}\mathbf{j}\right] \times \cos\phi, \tag{2}$$

where u, v, and ξ represent the zonal and meridional wind speed and the vertical component of the vorticity, respectively, f is the Coriolis parameter, g is the gravitational acceleration, h indicates the horizontal component, $\mathbf{i}$ and $\mathbf{j}$ represent the zonal and meridional unit

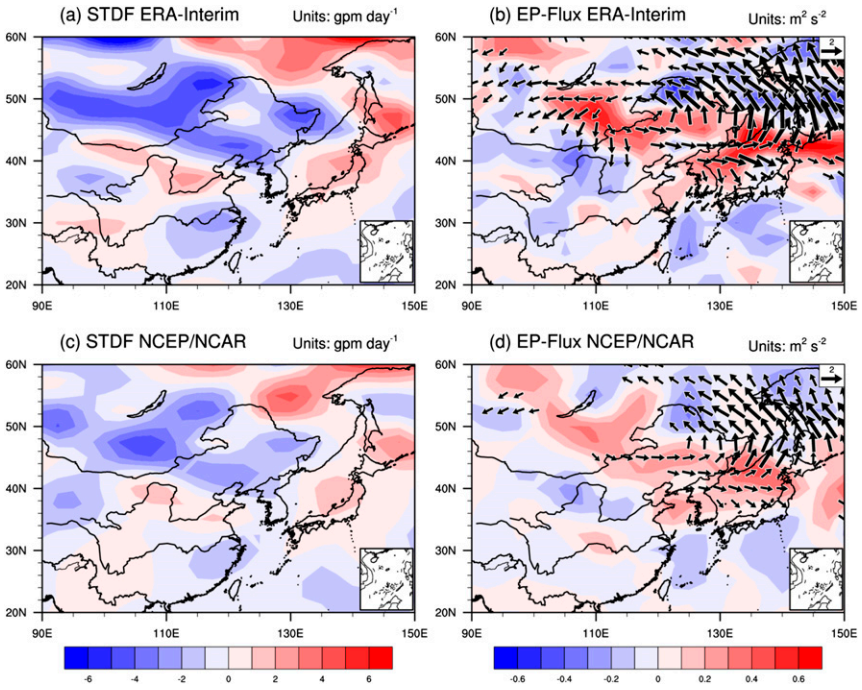

FIG. 7. Regressions of summer mean 300-hPa (a),(c) STDF (gpm day^{-1}; shading) and (b),(d) EP flux (m^2 s^{-2}; vectors) and EP flux divergence (10^{-5} m s^{-2}; shading) onto the normalized EAMC time series based on (left) ERA-Interim and (right) NCEP–NCAR reanalyses.

vector, and ϕ is the latitude. Here, the prime sign indicates a synoptic-scale disturbance obtained from the 2.5–6-day Butterworth bandpass filter (Murakami 1979), while the bar indicates a monthly average of the variables.

Figure 7 presents the results for the relevant physical parameters of the synoptic-scale transient wave activity that were derived from the regression of the normalized number of cyclones in the representative areas. Figure 7a shows the dynamic contribution of the synoptic-scale transient wave to the geopotential tendency. A significant negative anomaly is evident in the region between eastern Mongolia to the south of Lake Baikal and northeastern China. This anomaly distribution is similar to the spatial pattern of the geopotential height anomaly as shown in Figs. 6e and 6f, which indicates that there is a close relationship between the negative anomaly of the geopotential height around Lake Baikal area and the synoptic-scale transient wave activity. The possible physical mechanism is that when the cyclone activity is strong, the cyclone dissipation is accompanied by a positive poleward flux of the eddy vorticity, leading to a positive vorticity anomaly to the north of the area of cyclone activity and hence the cyclonic circulation anomaly; moreover, the action of the Coriolis geostrophic deflection force causes the atmospheric mass to diverge outward, which forms an anomaly in the atmospheric geopotential height. Figure 7b shows that a divergence of the EP flux occurs in the regions from eastern Mongolia through northeastern China to the Sea of Japan, and its location corresponds to that of the cyclone dissipation. The dissipation of the cyclone is accompanied by the conversion of the energy of the synoptic-scale disturbance to the kinetic energy of mean flow. The westerly wind is accelerated in the area of EP flux divergence, and a low pressure and anomalous cyclonic circulation forms to the north of the area of cyclone activity.

The above analysis of relevant physical quantities of the synoptic-scale disturbance demonstrates that the abnormally strong cyclone activity can cause significant negative anomalies of sea level pressure and geopotential field near Lake Baikal through the poleward transport of the vorticity flux, resulting in anomalous cyclonic circulation in these areas, while the southerly anomaly to the southeast of the anomalous cyclonic circulation near Lake Baikal is favorable for the significant enhancement of EASM. The opposite situation occurs when the cyclone activity anomaly is weak, which usually causes the weakening of EASM.

5. Linkage between midlatitude cyclone anomaly and land surface nonuniform warming

The analysis presented above reveals the relationship between the midlatitude summer cyclone anomaly in

East Asia and EASM. However, what is the cause of the midlatitude cyclone anomaly in East Asia? In the general context of global warming, the changes of surface temperature over the Eurasian continent exhibit high spatial heterogeneity, which has the potential to alter the atmospheric baroclinicity and thus the cyclone activity. In this section, we investigate the possible linkage between the midlatitude cyclone and land surface nonuniform warming and attempt to explore one possible reason for the midlatitude summer cyclone anomaly in East Asia from the perspective of the nonuniform warming.

Because the cyclone activity decreased significantly after the early 1990s, we multiplied the normalized time series of the number of cyclones by −1 and performed a regression analysis of the surface temperature of the Eurasian continent. As shown in Fig. 8, except for the NCEP–NCAR reanalyses, which show cold anomalies in East Siberia, south of the Tibetan Plateau and north of India, the results from the four datasets all indicate large-scale anomalous warming of the Eurasian continent. The most significant anomalous warming appears in western Mongolia to the south of Lake Baikal. It suggests that the weakening of cyclone activity might be closely related to the significant nonuniform land surface warming.

Figure 9 shows the normalized time series of the average regional summer surface temperature in the vicinity of Lake Baikal (40°–60°N, 90°–120°E). The four datasets reflect consistent characteristics of the variations in the surface temperature; there is an obvious warming trend in the surface temperature from 1993 to 1997, and the surface temperature around Lake Baikal changed from relatively cold before 1993 to significantly warmer after 1997. The results of the moving Student's t test (Fig. 9b) indicate that for moving window lengths of 9 or 10 years, the decadal variations of the surface temperature near Lake Baikal occurred in 1993 and around 1997, respectively, both passing the significance test at the 1% level. Overall, the decadal warming of the land surface around the early 1990s is generally consistent with the weakening of the cyclone. However, it is noted that the significant changing point of land surface temperature happened in 1997, which is not exactly the same as the changing point of the cyclone. Although the land surface warming can provide some explanation on the anomalous cyclone activities, other impact factors should also be examined to better understand the reasons for the anomalous cyclone activity. In addition, the feedback of the anomalous cyclone activity on the change of the land surface temperature deserves further investigation in the future.

To further verify the linkage between the midlatitude cyclone anomaly and land surface nonuniform warming, we explored the basic features of the land surface temperature between weak and strong cyclone activities. In comparison with 1979–93, the average land surface temperature during summer in the mid- to high latitudes over the Eurasian continent is warmer for the period 1994–2013; the spatial distribution depicted in Fig. 10 shows that this decadal warming is nonuniform and that the strongest warming center is located in Mongolia to the southwest of Lake Baikal, where the increase in temperature is more than 1.5°C. The warming trend is weakest in western Siberia, and the ERA-Interim and CRU data show cooling of approximately 0.4°C to the north of India. The results of the CRU data indicate that compared with 1979–93, the average warming around Lake Baikal area from 1994 to 2013 reaches about 1°C, while the overall warming of the Eurasian continent is merely 0.7°C.

The surface thermal anomaly can affect the cyclone activity by altering the atmospheric baroclinicity in the area of cyclone generation. To more directly reflect the impact of the variation in atmospheric baroclinicity on the cyclone activity, we calculated the maximum Eady growth rate σ_{BI} between 850 and 700 hPa, $\sigma_{\mathrm{BI}} = 0.31 f(\partial|\overline{\mathbf{V}}|/\partial z)N^{-1}$ (where f is the Coriolis parameter, N is the Brunt–Väisälä frequency, $\overline{\mathbf{V}}$ is the time-averaged horizontal wind speed, and z is the vertical height), which is used to characterize the low-level atmospheric baroclinicity. Larger values of σ_{BI} indicate stronger baroclinicity of the atmosphere, which favors the generation and development of cyclones. This index has been widely applied in the research of the atmospheric baroclinicity (Eady 1949; Lindzen et al. 1980). Figure 11a shows the spatial distribution of the temporal correlation between the surface temperature near Lake Baikal and the maximum Eady growth rate. The two parameters exhibit a significant negative correlation in the Mongolian area near the region of cyclone generation but a positive correlation in the region north and west of Lake Baikal; this is related to the location of the strongest warming center of the surface temperature (Fig. 10). Based on the principle of thermal wind and the definition of atmospheric baroclinicity, the north–south temperature gradient increases to the north of the warming center, and the atmospheric baroclinicity increases; the north–south temperature gradient decreases to the south, and the atmospheric baroclinicity weakens. Further analysis indicates that the variation in the atmospheric baroclinicity induced by the nonuniform heating of the land surface can have a significant impact on the cyclone activity. Figure 11b shows the spatial distribution of the atmospheric baroclinicity index anomaly derived from the regression of the normalized number of cyclones. The atmospheric

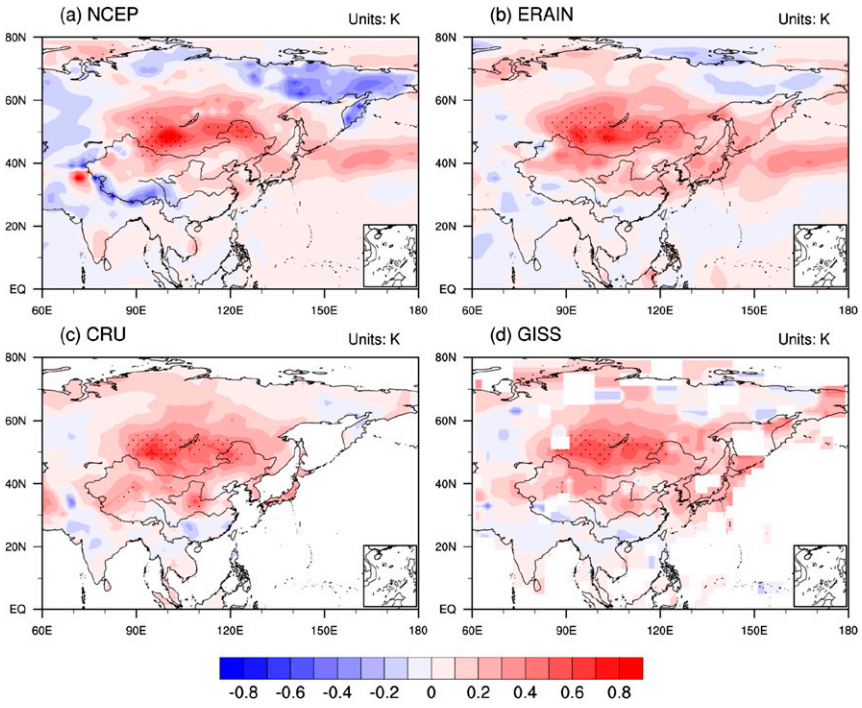

FIG. 8. Regressions of summer surface air temperature anomalies (K) over Eurasian continent onto the normalized EAMC time series (multiplied by −1) based on (a) NCEP–NCAR reanalyses, (b) ERA-Interim, (c) CRU, and (d) NASA GISS, in which black dots denote the regions where the regression is statistically significant at the 1% level.

baroclinicity in the midlatitudes over the Eurasian continent exhibits a clear negative anomaly that corresponds to the abnormal weakening of cyclone activity. This significant negative anomaly of the atmospheric baroclinicity is mainly located near 40°N and extends eastward from west of the Mongolian Plateau to northeastern China. The weakening of cyclone activity after the early 1990s can be attributed to the significant weakening of the atmospheric baroclinicity in this region. Because of the nonuniformity of land surface warming of the Eurasian continent, the largest warming center appears to the west of Lake Baikal, which leads to a decrease in the atmospheric baroclinicity to the south and eventually results in the weakening of the midlatitude cyclone activity.

6. Conclusions and discussion

Based on the 4-times-daily ERA-Interim sea level pressure data, we used an objective identification and

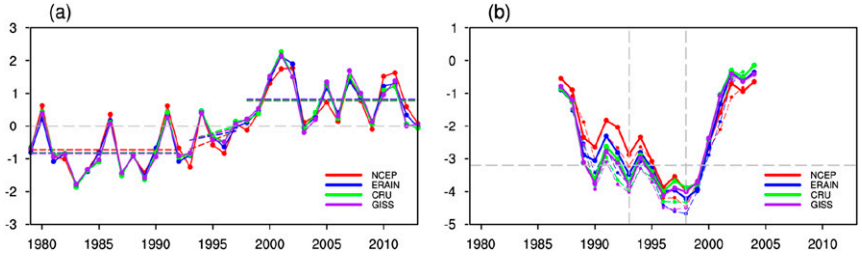

FIG. 9. (a) Normalized time series of summer mean surface air temperature anomalies around Lake Baikal (40°–60°N, 90°–120°E), in which the horizontal dashed lines indicate the average during 1979–92 and 1998–2013. (b) Statistics of the moving Student's *t* test for the surface air temperature during the period 1979–2013, in which solid and dashed marked lines are results for a 9- and 10-yr window, respectively. Horizontal dashed gray lines indicate the values passing statistical test at the 1% significance level and vertical dashed gray line shows significant abrupt changing point.

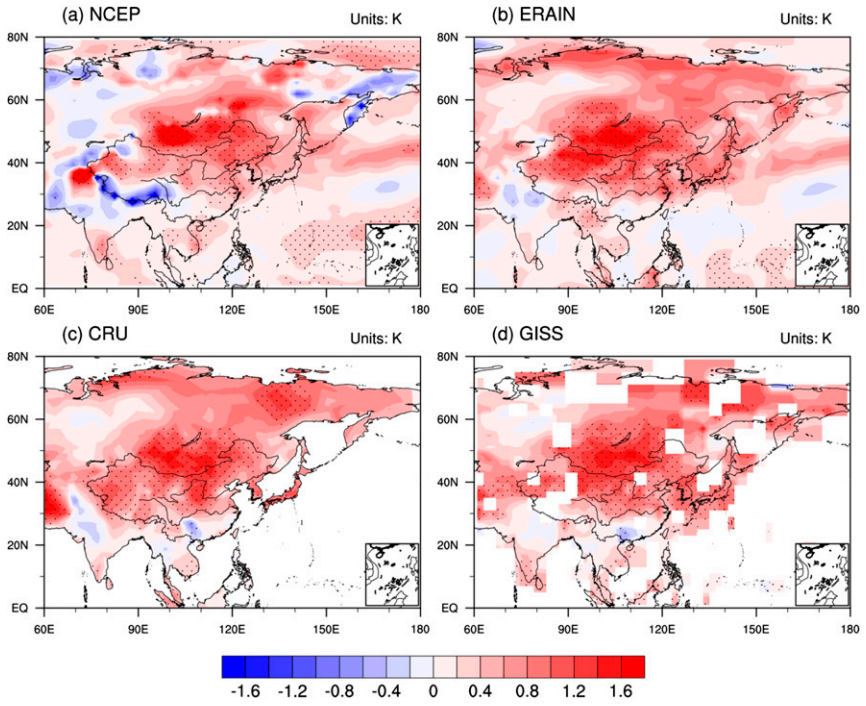

FIG. 10. Differences of summer mean surface air temperature (K) over Eurasian continent between the periods of 1994–2013 and 1979–93 based on (a) NCEP–NCAR reanalyses, (b) ERA-Interim, (c) CRU, and (d) NASA GISS. Black dots denote regions where the composite analysis is statistically significant at the 1% level.

tracking algorithm of the cyclone to attain a database that reflects the cyclone activity in the Northern Hemisphere. The basic characteristics of anomalous variations of the midlatitude cyclone activity in East Asia during summer were analyzed over the past 35 years, and the possible mechanisms by which the anomalous cyclone activity affects EASM were explored subsequently. We also investigated the possible reasons for the anomalous midlatitude summer cyclone activity in East Asia from the perspective of nonuniform surface warming of the Eurasian continent.

Results indicate that central Mongolia is the key area with not only the most frequent cyclone activity but also the strongest variability of the cyclone activity. A

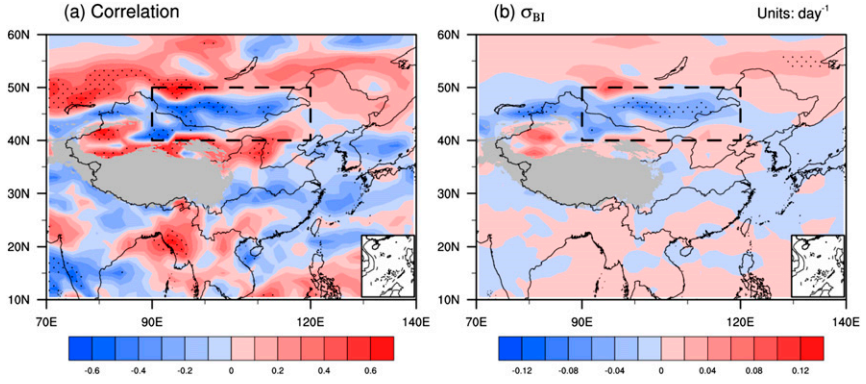

FIG. 11. (a) Correlation coefficients between low-level (between 850 and 700 hPa) atmospheric baroclinicity and the surface air temperature around Lake Baikal in the period 1979–2013 over the Eurasian continent. (b) Regression of the atmospheric baroclinicity anomaly (day^{-1}) onto the normalized EAMC time series, in which black dots denote regions where the correlation and regression are statistically significant at the 5% level.

significant weakening trend and a decadal variation of the cyclone activity occurred in this area between 1979 and 2013. The decadal transition occurred in the early 1990s, after which the cyclone activity became weaker.

Further analysis indicates that there is a significant positive correlation between the midlatitude cyclone activity over East Asia and the decadal variation of EASM represented by EASM-PC2; when the midlatitude summer cyclone activity in East Asia is strong (weak), EASM is strong (weak). Over the last 20 years, the weakening of the midlatitude summer cyclone activity in East Asia is closely correlated with the weakening of EASM. Through the analysis of relevant physical parameters of the synoptic-scale wave, we demonstrated that abnormally strong cyclone activity can lead to the occurrence of significant negative anomalies of sea level pressure and geopotential heights near Lake Baikal through the poleward vorticity flux transport, which results in anomalous cyclonic circulation in these areas. The southerly anomaly to the southeast of the anomalous cyclonic circulation near Lake Baikal is conducive to the significant intensification of EASM. The opposite situation occurs when the cyclone activity is weak, which usually weakens EASM.

It is also found in this study that the weakening of the cyclone activity after the early 1990s is closely related to the nonuniform land surface warming over the Eurasia. The significant warming in western Mongolia can cause evident weakening of the north–south temperature gradient and the atmospheric baroclinicity to its south, which eventually results in the weakening of the midlatitude cyclone activity during summer in East Asia.

By analyzing the cyclone activity and the relevant physical parameters of the synoptic-scale transient wave, we proposed one possible mechanism by which the midlatitude synoptic processes affect EASM. However, the decadal variation of EASM is affected by many factors; a more thorough analysis merits further investigation in the future.

In addition, recent studies have suggested that summer midlatitude cyclone activity has weakened significantly over the Northern Hemisphere since 1979 and also pointed out that CMIP5 models project a weakening in cyclone activity under global warming (Coumou et al. 2015; Chang et al. 2016). Here we focused on the impacts of the midlatitude cyclone activity over East Asia induced by nonuniform warming of the Eurasian continent on EASM. Both of these researches are consistent with a downward trend of cyclone activity or midlatitude circulation in connection with the temperature change. However, it is noted that the significant changing point of land surface temperature happened in 1997, which is not exactly the same as the changing point of the cyclone. Other impact factors should also be examined to better understand the reasons for the anomalous cyclone activity in the future.

Acknowledgments. This study has been jointly supported by the National Natural Science Foundation of China (41230422, 41625019), the Special Funds for Public Welfare of China (GYHY 201206017), the program for New Century Excellent Talents in University (NCET) of the Ministry of Education of China, the Natural Science Foundation of Jiangsu Province of China under Grant BK20130047, and the project funded by the Priority Academic Program Development of Jiangsu Higher Education Institutions (PAPD). (The ERA-Interim dataset is available at http://apps.ecmwf.int/datasets/, the NCEP–NCAR reanalyses data are available at http://www.esrl.noaa.gov/psd/, the CRU datasets are available at http://www.cru.uea.ac.uk/data/, the NASA GISS datasets are available at http://data.giss.nasa.gov/gistemp/, and the GPCP datasets are available at http://www.esrl.noaa.gov/psd/data/gridded/data.gpcp.html.)

REFERENCES

Adler, R. F., and Coauthors, 2003: The version-2 Global Precipitation Climatology Project (GPCP) monthly precipitation analysis (1979–present). *J. Hydrometeor.*, **4**, 1147–1167, doi:10.1175/1525-7541(2003)004<1147:TVGPCP>2.0.CO;2.

Chang, C.-P., Y. Zhang, and T. Li, 2000a: Interannual and interdecadal variation of the East Asian summer monsoon rainfall and tropical SSTs. Part I: Roles of the subtropical ridge. *J. Climate*, **13**, 4310–4325, doi:10.1175/1520-0442(2000)013<4310:IAIVOT>2.0.CO;2.

——, ——, and ——, 2000b: Interannual and interdecadal variation of the East Asian summer monsoon rainfall and tropical SSTs. Part II: Meridional structure of the monsoon. *J. Climate*, **13**, 4326–4340, doi:10.1175/1520-0442(2000)013<4326:IAIVOT>2.0.CO;2.

Chang, E. K. M., Y. Guo, and X. Xia, 2012: CMIP5 multimodel ensemble projection of storm track change under global warming. *J. Geophys. Res.*, **117**, D23118, doi:10.1029/2012JD018578.

——, C.-G. Ma, C. Zheng, and A. M. W. Yau, 2016: Observed and projected decrease in Northern Hemisphere extratropical cyclone activity in summer and its impacts on maximum temperature. *Geophys. Res. Lett.*, **43**, 2200–2208, doi:10.1002/2016GL068172.

Chen, W., and R. Y. Lu, 2014: A decadal shift of summer surface air temperature over northeast Asia around the mid-1990s. *Adv. Atmos. Sci.*, **31**, 735–742, doi:10.1007/s00376-013-3154-4.

Coumou, D., J. Lehmann, and J. Beckmann, 2015: The weakening summer circulation in the Northern Hemisphere mid-latitudes. *Science*, **348**, 324–327, doi:10.1126/science.1261768.

Dee, D. P., and Coauthors, 2011: The ERA-Interim reanalysis: Configuration and performance of the data assimilation system. *Quart. J. Roy. Meteor. Soc.*, **137**, 553–597, doi:10.1002/qj.828.

Ding, Q., and B. Wang, 2007: Intraseasonal teleconnection between the summer Eurasian wave train and the Indian monsoon. *J. Climate*, **20**, 3751–3767, doi:10.1175/JCLI4221.1.

Ding, Y. H., and J. C. L. Chan, 2005: The East Asian summer monsoon: An overview. *Meteor. Atmos. Phys.*, **89**, 117–142, doi:10.1007/s00703-005-0125-z.

——, Z. Y. Wang, and Y. Sun, 2008: Inter-decadal variation of the summer precipitation in east China and its association with decreasing Asian summer monsoon. Part I: Observed evidences. *Int. J. Climatol.*, **28**, 1139–1161, doi:10.1002/joc.1615.

——, Y. Sun, and Z. Y. Wang, 2009: Inter-decadal variation of the summer precipitation in China and its association with decreasing Asian summer monsoon. Part II: Possible causes. *Int. J. Climatol.*, **29**, 1926–1944, doi:10.1002/joc.1759.

Eady, E. T., 1949: Long waves and cyclone waves. *Tellus*, **1A**, 33–52, doi:10.1111/j.2153-3490.1949.tb01265.x.

Fujinami, H., and T. Yasunari, 2009: The effects of midlatitude waves over and around the Tibetan Plateau on submonthly variability of the East Asian summer monsoon. *Mon. Wea. Rev.*, **137**, 2286–2304, doi:10.1175/2009MWR2826.1.

Hansen, J., M. Sato, R. Ruedy, K. Lo, D. W. Lea, and M. Medina-Elizade, 2006: Global temperature change. *Proc. Natl. Acad. Sci. USA*, **103**, 14 288–14 293, doi:10.1073/pnas.0606291103.

——, R. Ruedy, M. Sato, and K. Lo, 2010: Global surface temperature change. *Rev. Geophys.*, **48**, RG4004, doi:10.1029/2010RG000345.

Harris, I., P. D. Jones, T. J. Osborn, and D. H. Lister, 2014: Updated high-resolution grids of monthly climatic observations—The CRU TS3.10 dataset. *Int. J. Climatol.*, **34**, 623–642, doi:10.1002/joc.3711.

He, J. H., Z. W. Wu, Z. H. Jiang, C. S. Miao, and G. R. Han, 2007a: ''Climate effects'' of the northeast cold vortex and its influence on meiyu. *Chin. Sci. Bull.*, **52**, 671–679, doi:10.1007/s11434-007-0053-z.

——, J. H. Ju, Z. P. Wen, J. M. Lu, and Q. H. Jin, 2007b: A review of recent advances in research on Asian monsoon in China. *Adv. Atmos. Sci.*, **24**, 972–992, doi:10.1007/s00376-007-0972-2.

Hsu, H.-H., T. J. Zhou, and J. Matsumoto, 2014: East Asian, Indochina and western North Pacific summer monsoon—An update. *Asia-Pac. J. Atmos. Sci.*, **50**, 45–68, doi:10.1007/s13143-014-0027-4.

Huang, R. H., L. T. Zhou, and W. Chen, 2003: The progresses of recent studies on the variabilities of the East Asian monsoon and their causes. *Adv. Atmos. Sci.*, **20**, 55–69, doi:10.1007/BF03342050.

——, J. L. Chen, L. Wang, and Z. D. Lin, 2012: Characteristics, processes, and causes of the spatio-temporal variabilities of the East Asian monsoon system. *Adv. Atmos. Sci.*, **29**, 910–942, doi:10.1007/s00376-012-2015-x.

Huang, Y. L., H. S. Chen, W. Jiang, B. Xu, and Z. X. Li, 2015: Multi-spatial modes of East Asian summer monsoon activity: Comparative analysis of various reanalysis data (in Chinese). *Chin. J. Atmos. Sci.*, **39**, 145–160.

Kalnay, E., and Coauthors, 1996: The NCEP/NCAR 40-Year Reanalysis Project. *Bull. Amer. Meteor. Soc.*, **77**, 437–471, doi:10.1175/1520-0477(1996)077<0437:TNYRP>2.0.CO;2.

Kwon, M., J.-G. Jhun, and K.-J. Ha, 2007: Decadal change in East Asian summer monsoon circulation in the mid-1990s. *Geophys. Res. Lett.*, **34**, L21706, doi:10.1029/2007GL031977.

Lau, N.-C., 1988: Variability of the observed midlatitude storm tracks in relation to low-frequency changes in the circulation pattern. *J. Atmos. Sci.*, **45**, 2718–2743, doi:10.1175/1520-0469(1988)045<2718:VOTOMS>2.0.CO;2.

——, and E. O. Holopainen, 1984: Transient eddy forcing of the time-mean flow as identified by geopotential tendencies. *J. Atmos. Sci.*, **41**, 313–328, doi:10.1175/1520-0469(1984)041<0313:TEFOTT>2.0.CO;2.

——, and M. J. Nath, 1991: Variability of the baroclinic and barotropic transient eddy forcing associated with monthly changes in the midlatitude storm tracks. *J. Atmos. Sci.*, **48**, 2589–2613, doi:10.1175/1520-0469(1991)048<2589:VOTBAB>2.0.CO;2.

Lehmann, J., D. Coumou, K. Frieler, A. V. Eliseev, and A. Levermann, 2014: Future changes in extratropical storm tracks and baroclinicity under climate change. *Environ. Res. Lett.*, **9**, 084002, doi:10.1088/1748-9326/9/8/084002.

Lindzen, R. S., B. Farrell, and K.-K. Tung, 1980: The concept of wave overreflection and its application to baroclinic instability. *J. Atmos. Sci.*, **37**, 44–63, doi:10.1175/1520-0469(1980)037<0044:TCOWOA>2.0.CO;2.

McCabe, G. J., M. P. Clark, and M. C. Serreze, 2001: Trends in Northern Hemisphere surface cyclone frequency and intensity. *J. Climate*, **14**, 2763–2768, doi:10.1175/1520-0442(2001)014<2763:TINHSC>2.0.CO;2.

Murakami, M., 1979: Large-scale aspects of deep convective activity over the GATE area. *Mon. Wea. Rev.*, **107**, 994–1013, doi:10.1175/1520-0493(1979)107<0994:LSAODC>2.0.CO;2.

Murray, R. J., and I. Simmonds, 1991a: A numerical scheme for tracking cyclone centres from digital data. Part I: Development and operation of the scheme. *Aust. Meteor. Mag.*, **39**, 155–166.

——, and ——, 1991b: A numerical scheme for tracking cyclone centres from digital data. Part II: Application to January and July general circulation model simulations. *Aust. Meteor. Mag.*, **39**, 167–180.

Park, H.-S., B. R. Lintner, W. R. Boos, and K.-H. Seo, 2015: The effect of midlatitude transient eddies on monsoonal southerlies over eastern China. *J. Climate*, **28**, 8450–8465, doi:10.1175/JCLI-D-15-0133.1.

Qi, L., and Y. Q. Wang, 2012: Changes in the observed trends in extreme temperatures over China around 1990. *J. Climate*, **25**, 5208–5222, doi:10.1175/JCLI-D-11-00437.1.

Seo, K.-H., J.-H. Son, S.-E. Lee, and T. Tomita, 2012: Mechanisms of an extraordinary East Asian summer monsoon event in July 2011. *Geophys. Res. Lett.*, **39**, L05704, doi:10.1029/2011GL050378.

——, ——, J.-Y. Lee, and H.-S. Park, 2015: Northern East Asian monsoon precipitation revealed by airmass variability and its prediction. *J. Climate*, **28**, 6221–6233, doi:10.1175/JCLI-D-14-00526.1.

Simmonds, I., R. J. Murray, and R. M. Leighton, 1999: A refinement of cyclone tracking methods with data from FROST. *Aust. Meteor. Mag.*, **48**, 35–49.

Song, L., L. Wang, W. Chen, and Y. Zhang, 2016: Intraseasonal variation of the strength of the East Asian trough and its climatic impacts in boreal winter. *J. Climate*, **29**, 2557–2577, doi:10.1175/JCLI-D-14-00834.1.

Tao, S. Y., and L. X. Chen, 1987: A review of recent research on the East Asian summer monsoon in China. *Monsoon Meteorology*, C.-P. Chang and T. N. Krishnamurti, Eds., Clarendon, 60–92.

Tomita, K.-H., T. Yamaura, and T. Hashimoto, 2011: Interannual variability of the baiu season near Japan evaluated from the equivalent potential temperature. *J. Meteor. Soc. Japan*, **89**, 517–537, doi:10.2151/jmsj.2011-507.

Trenberth, K. E., 1986: An assessment of the impact of transient eddies on the zonal flow during a blocking episode using localized Eliassen–Palm flux diagnostics. *J. Atmos. Sci.*, **43**, 2070–2087, doi:10.1175/1520-0469(1986)043<2070:AAOTIO>2.0.CO;2.

Ulbrich, U., G. C. Leckebusch, and J. G. Pinto, 2009: Extra-tropical cyclones in the present and future climate: A review. *Theor. Appl. Climatol.*, **96**, 117–131, doi:10.1007/s00704-008-0083-8.

Wang, B., R. G. Wu, and X. H. Fu, 2000: Pacific–East Asian teleconnection: How does ENSO affect East Asian climate? *J. Climate*, **13**, 1517–1536, doi:10.1175/1520-0442(2000)013<1517:PEATHD>2.0.CO;2.

——, Z. Wu, J. Li, J. Liu, C.-P. Chang, Y. Ding, and G. Wu, 2008: How to measure the strength of the East Asian summer monsoon? *J. Climate*, **21**, 4449–4463, doi:10.1175/2008JCLI2183.1.

Wang, H. J., 2001: The weakening of the Asian monsoon circulation after the end of 1970's. *Adv. Atmos. Sci.*, **18**, 376–386, doi:10.1007/BF02919316.

Wang, X. M., P. M. Zhai, and C. C. Wang, 2009: Variations in extratropical cyclone activity in northern East Asia. *Adv. Atmos. Sci.*, **26**, 471–479, doi:10.1007/s00376-009-0471-8.

Wu, B. Y., K. Yang, and R. H. Zhang, 2009a: Eurasian snow cover variability and its association with summer rainfall in China. *Adv. Atmos. Sci.*, **26**, 31–44, doi:10.1007/s00376-009-0031-2.

——, R. H. Zhang, B. Wang, and R. D'Arrigo, 2009b: On the association between spring Arctic sea ice concentration and Chinese summer rainfall. *Geophys. Res. Lett.*, **36**, L09501, doi:10.1007/s00376-009-9009-3.

Wu, G. X., J. Y. Mao, A. M. Duan, and Q. Zhang, 2004: Recent progress in the study on the impacts of Tibetan Plateau on Asian summer climate (in Chinese). *Acta Meteor. Sin.*, **62**, 528–540.

Wu, R. G., 2002: A mid-latitude Asian circulation anomaly pattern in boreal summer and its connection with the Indian and East Asian summer monsoons. *Int. J. Climatol.*, **22**, 1879–1895, doi:10.1002/joc.845.

——, Z. P. Wen, S. Yang, and Y. Q. Li, 2010: An interdecadal change in southern China summer rainfall around 1992/93. *J. Climate*, **23**, 2389–2403, doi:10.1175/2009JCLI3336.1.

Zhang, L. X., and T. J. Zhou, 2015: Decadal change of East Asian summer tropospheric temperature meridional gradient around the early 1990s. *Sci. China Earth Sci.*, **58**, 1609–1622, doi:10.1007/s11430-015-5117-3.

Zhang, R. H., and Z. Y. Zuo, 2011: Impact of spring soil moisture on surface energy balance and summer monsoon circulation over East Asia and precipitation in east China. *J. Climate*, **24**, 3309–3322, doi:10.1175/2011JCLI4084.1.

Zhang, Y. X., Y. H. Ding, and Q. P. Li, 2012a: A climatology of extratropical cyclones over East Asia during 1958–2011. *Acta Meteor. Sin.*, **26**, 261–277, doi:10.1007/s13351-012-0301-2.

——, ——, and ——, 2012b: Cyclogenesis frequency changes of extratropical cyclones in the Northern Hemisphere and East Asia revealed by ERA40 reanalysis data (in Chinese). *Meteor. Mon.*, **38**, 646–656.

Zhu, C. W., B. Wang, W. H. Qian, and B. Zhang, 2012: Recent weakening of northern East Asian summer monsoon: A possible response to global warming. *Geophys. Res. Lett.*, **39**, L09701, doi:10.1029/2012GL051155.